**Zeitschrift:** IABSE reports = Rapports AIPC = IVBH Berichte

**Band:** 54 (1987)

**Artikel:** Constitutive equations of a cracked reinforced concrete panel

Autor: Tanabe, Tadaaki / Yoshikawa, Hiromichi

**DOI:** https://doi.org/10.5169/seals-41913

## Nutzungsbedingungen

Die ETH-Bibliothek ist die Anbieterin der digitalisierten Zeitschriften auf E-Periodica. Sie besitzt keine Urheberrechte an den Zeitschriften und ist nicht verantwortlich für deren Inhalte. Die Rechte liegen in der Regel bei den Herausgebern beziehungsweise den externen Rechteinhabern. Das Veröffentlichen von Bildern in Print- und Online-Publikationen sowie auf Social Media-Kanälen oder Webseiten ist nur mit vorheriger Genehmigung der Rechteinhaber erlaubt. Mehr erfahren

## **Conditions d'utilisation**

L'ETH Library est le fournisseur des revues numérisées. Elle ne détient aucun droit d'auteur sur les revues et n'est pas responsable de leur contenu. En règle générale, les droits sont détenus par les éditeurs ou les détenteurs de droits externes. La reproduction d'images dans des publications imprimées ou en ligne ainsi que sur des canaux de médias sociaux ou des sites web n'est autorisée qu'avec l'accord préalable des détenteurs des droits. En savoir plus

### Terms of use

The ETH Library is the provider of the digitised journals. It does not own any copyrights to the journals and is not responsible for their content. The rights usually lie with the publishers or the external rights holders. Publishing images in print and online publications, as well as on social media channels or websites, is only permitted with the prior consent of the rights holders. Find out more

**Download PDF:** 16.11.2025

ETH-Bibliothek Zürich, E-Periodica, https://www.e-periodica.ch



# **Constitutive Equations of a Cracked Reinforced Concrete Panel**

Equations constitutives d'un panneau en béton armé fissuré Werkstoffbeziehungen für eine gerissene Stahlbetonscheibe

Tadaaki TANABE Professor Nagoya University Nagoya, Japan



Tadaaki Tanabe, born in 1940, received his Dr. of Eng. at the University of Tokyo. After ten years research work in dams and RC structures of nuclear power stations, he joined the Nagoya University in 1981, was promoted to full Professor in 1984, and was engaged in the research of aseismic design and the thermal stress control of RC structures.



Hiromichi Yoshikawa, born in 1952, received his Dr. of Eng. at the University of Tokyo, involved in research work on the thermal stress analysis of massive concrete, analytical modelling of reinforced concrete members and finite element analysis of RC structures.

Hiromichi YOSHIKAWA Senior Research Eng. Hazamagumi Co., Ltd. Yono-Shi, Saitama, Japan

#### SUMMARY

Constitutive equations of composite materials of concrete and reinforcement in a twodimensional stress field are developed using damage and reinforcement tensors. The damage tensors are derived for the displacement fields of the frictionless mode at a crack, the contact frictional mode at a crack, and the mixed mode of both from the crack strains which are derived for each displacement field. The experimental results are compared with the theoretical calculations and a reasonable agreement is obtained.

#### RÉSUMÉ

Les équations constitutives des matériaux composites de béton et d'armatures sont établies pour un champ de contraintes bi-dimensionnelles, en utilisant les vecteurs de dommage et de renforcement. Les vecteurs de dommage sont obtenus à partir des champs de déplacement dûs à l'évolution d'une fissure sans friction, à l'évolution d'une fissure avec friction de contact, et à un mode mixte des deux mentionnés précédamment, à partir des contraintes de fissure qui sont obtenues pour chaque champ de déplacement. Les résultats expérimentaux sont comparés avec les calculs théoriques et une bonne concordance est obtenue.

#### ZUSAMMENFASSUNG

Werkstoffbeziehungen von Verbundmaterialien aus Beton und Bewehrung in der zweidimensionalen Spannungsfläche werden entwickelt, wobei von Schadens- und Verstärkungstensoren Gebrauch gemacht wird. Die Schadenstensoren werden für das Verschiebungsfeld von reibungslosen Rissen entwickelt, für den Riss mit Reibung und für gemischte Beanspruchung aus Rissöffnung und Rissverschiebung. Experimente werden mit der Theorie verglichen, wobei befriedigende Ubereinstimmung erreicht wird.



### 1. INTRODUCTION

The crack strain method in FEM analysis of a reinforced concrete structure is considered to be a very powerful means to incorporate material nonlinearities of various kinds in calculations. Crack strain in a discontinuous solid is defined in various ways. Powell, Villiers, and Litton [1] as well as Bazant and Gambaroba [2] defined crack strains as the crack width or crack slip divided by the average crack spacing, and expressed total strains as the sum of elastic strains and crack strains. Tanabe and Yamashita have treated a single crack by crack strain expressing it in e function [3]. Yoshikawa and Tanabe [4] defined crack strain in terms of delta function and extended to the case of tension stiffness formulation of reinforced concrete members, showing that crack strain so defined expresses bond slip between reinforcement and concrete.

On the other hand, crack strain has a natural relation to the damage tensor, which expresses the rate of damage of material from the intact condition. The damage tensor expresses material nonlinearity in explicit and simple form which enables the straightforward construction of the nonlinear constitutive equations in a comparatively simple way. In this paper, the fourth rank damage tensor is defined in terms of crack strain and the reinforcement tensor is defined in terms of stress increase due to the reinforcement. The general constitutive equations for the composite material made up of reinforcement and concrete are developed for a two dimensional stress field using these tensors. However, our attention will be limited to monotolic loading, with unloading and reloading excluded.

## 2.DEFINITION OF THE DAMAGE TENSOR FROM THE CRACK STRAINS

The damage tensor of the fourth rank may be defined in the following form to write stress reduction from the intact condition.

$$\Delta \sigma_{ij} = -Q_{ijpq}^{p} D_{pqmn} \varepsilon_{mn} \tag{2.1}$$

where  $^{A}\sigma_{ij}$  is the reduction of the nominal stress due to damage in the solid from the intact condition. As  $^{Q}_{ij\,p\,q}=^{Q}_{j\,ip\,q}=^{Q}_{j\,iq\,p}=^{Q}_{i\,j\,q\,p}$ , matrix expression for Eq.(2.1) is written as

$$\{ \Delta \sigma \} = -(\mathcal{Q})_{\mathcal{R}} \{ \mathcal{D} \}_{\mathcal{C}} \{ \mathcal{E} \} \tag{2.2}$$

Similarly, the reinforcement tensor may be written in terms of stress increase from the intact condition due to the reinforcement in concrete as

$$\Delta\sigma_{ij} = \Omega^{\kappa}_{ijpq} D_{pqmn} \varepsilon_{mn} \tag{2.3}$$

Eq.(2.3) is written in matrix form as

$$\{\Delta\sigma\} = (\Omega)_{\varepsilon} \{D\}_{\varepsilon} \{\varepsilon\} \tag{2.4}$$

Using Eq.(2.1) and Eq.(2.3), the general constitutive equation can be derived as

$$\{\sigma\} = (I - \mathcal{Q}_{p_1} - \mathcal{Q}_{p_2} - \dots + \mathcal{Q}_{p_1} + \mathcal{Q}_{p_2} + \dots) \{D\}_c \{\varepsilon\}$$

$$(2.5)$$

Stress reduction in concrete from the intact condition is written with the crack strain,  $\{\epsilon\}_{cr}$ , in the following form as well,

$$\{\Delta\sigma\} = -(D)_c \{\varepsilon\}_{cr} \tag{2.6}$$

Substitution of Eq.(2.6) into Eq.(2.2) yields



$$\{\varepsilon\}_{cr} = [D]_c^{-1} [Q]_p [D]_c \{\varepsilon\}$$
(2.7)

Hence, if  $\{\varepsilon\}_{cr}$  or stress reduction  $\{A\sigma\}$  is obtained, the  $\{\Omega\}$  can be derived. In other words, if  $\{\varepsilon\}_{cr}$  is obtained in terms of total strain in such a way that

$$\{\varepsilon\}_{cr} = (\Lambda)\{\varepsilon\} \tag{2.8}$$

then the damage tensor is obtained as

$$(Q)_{p} = (D)_{c} (A) (D)_{c}^{-1}$$
(2.9)

Similarly if the stress increase due to reinforcement is given in terms of total strain in such a way that

$$\{\Delta\sigma\} = \{\phi\} \{\varepsilon\},\tag{2.10}$$

the reinforcement tensor is obtained as

$$(\mathcal{Q})_{R} = (\phi) (D)_{C}^{-1}$$

$$(2.11)$$

The form of Eq.(2.5) is directly accommodated in a usual FEM program as the initial strain problem or the initial stress problem.

3.TENSION STIFFNESS FORMULATION IN A TWO DIMENSIONAL STRESS FIELD USING CRACK STRAINS

It is known that displacements of a reinforced concrete panel subjected to inplane loads are highly dependent on the bond characteristics between steel and concrete, the frictional characteristics at cracks, and the material nonlinearities of concrete and steel. In this section, the analytical model for calculating the effect of bond characteristics or tension stiffness effects on deformation is presented. Bond characteristics between steel and concrete are directly related to crack spacing and crack width. For the rigorous analysis of those, we need a fracture theory of concrete. However, we simplify the problem by the assumption that concrete is a linear elastic brittle fracture material in tension and the solution is obtained. Its solution is then modified by coefficients which reflect nonlinearity of the material characteristics.

The experimentally observed relation between the maximum crack spacing, lmax, and the minimum spacing, lmin, for a uniaxially reinforced concrete member suggests that they have a relation of

$$\ell_{max} = C \cdot \ell_{min} \tag{3.1}$$

where C is constant. For instance, Goto has proposed that C=2 [5]. Osaka et.al. proposed that C=4 [6].

Supposing that a new crack initiates when the maximum tensile stress reaches the tensile strength of the concrete, ft, and that the crack spacing satisfies the Eq.(3.1), the upper envelop curve of lmax and the lower envelop curve of lmin is obtained uniquely for any arbitrary initial length of  $\ell$ , as the continuous function of applied stress, as shown in Fig.3.1. The function thus obtained decides the analytical expression of the relation between applied stress and crack strains.

If we assume the linear bond slip law for a uniaxially reinforced concrete



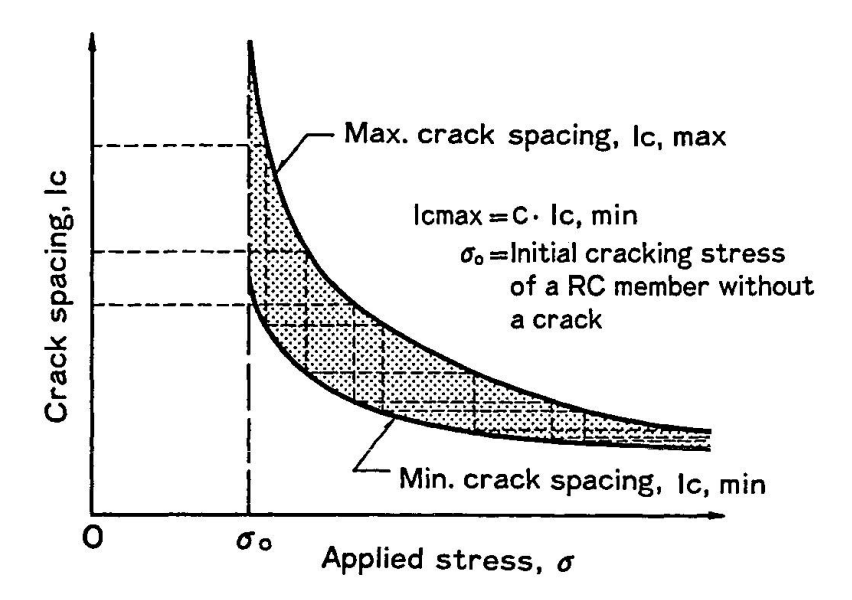


Fig. 3.1 Envelope Curves for the Maximum and the Minimum Crack Spacings

member, and the governing equation of bond stress, and bond slip relation as  $d^2g/dx^2-k$  g=0 [7], where g is the slip,  $k=(u/u_0)/(g/g_0)$ , and u.  $u_0$ .  $g_0$  are the bond stress, bond strength and the corresponding slip at the maximum bond strength, respectively, and that a crack initiates when concrete stress reaches concrete tensile strength, ft, the upper bound envelop curve is expressed as

$$\cos h(\ell_c/b_c) = \frac{\sigma}{\sigma - (1+np)f_t} \tag{3.2}$$

where  $\ell_c$  is half of the crack spacing,  $\sigma$  is the applied uniaxial stress, and be is the parameter that shows bond characteristics and is expressed as  $b_c = \left[ k \; u_0 s \, (1 + n p) / \, (g_0 A_S \, E_S) \, \right]^{-\frac{1}{2}}$  The notations n, p, s, and As, denote the ratio of the Young's Modulus of steel to that of concrete, steel ratio, bar diameter, and sectional area of a bar, respectively.

The lower envelop curve is obtained by substituting  $\mathcal{C} \cdot \ell_c$  in  $\ell_c$  of Eq(3.2). Crack strain  $\{\varepsilon\}_{cr}$  is defined as the crack width divided by the average crack spacing. As crack width,  $\delta_w$ , equals  $2\,b_c\,\tan h\,(\,\ell_c\,/\,b_c\,)\cdot\sigma/p\,E_s$ .

$$\varepsilon_{cr} = \lambda \frac{\sigma}{pE_s} \tag{3.3}$$

where  $\lambda = \tan h (\mu_c) / \mu_c$ ,  $\mu_c = \ell_c / b_c = \cos h^{-1} (\sigma / \{\sigma - (1 + np) \cdot f_t\})$ 

Now, the total strain is written as

$$\varepsilon = \left(\frac{\lambda + np}{1 + np}\right) \frac{\sigma}{E_s} \tag{3.4}$$

Hence tension stiffness is expressed by the parameter,  $\lambda$ ,  $(0 \le \lambda \le 1)$ . If  $\lambda = 0$ ,  $\varepsilon \operatorname{cr} = 0$  and full contribution to tension stiffness from concrete exists, while if  $\lambda = 1$ , then  $\varepsilon_{cr} = \sigma/E_s = \varepsilon_s$ , steel strain, and no contribution to tension stiffness from concrete exists. The effect of nonlinear characteristics of bond slip law is introduced now by the comparison of the solution with the experimental values. They show that better fitting is obtained if the crack spacing and stress relation is shifted from the upper bound envelop to the lower envelop curve with the increase of applied stress. This modification factor  $\beta$ , which is to be multiplied to the linear solution of crack spacing, is expressed

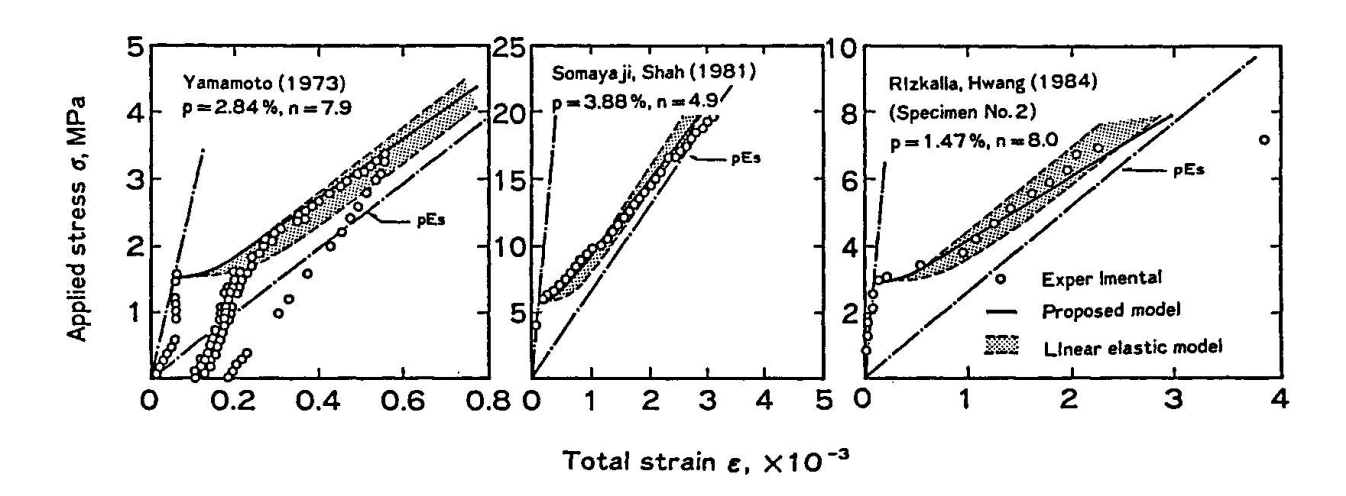


Fig.3.2 Applied Stress and Total Strain Relations in Uniaxial Tension Tests (Ref.8,9,10)

as Eq.(3.5), where fy is the yielding stress of a bar,

$$\beta = 1 - C_{s} \frac{\sigma - (1 + np) f_{t}}{p f_{y} - (1 + np) f_{t}}$$
(3.5)

and normalized crack spacing is given as

$$\mu = \ell_c / b_c = \beta \cos h^{-1} \left\{ \frac{\sigma}{\sigma - (1 + n\rho) f_t} \right\}$$
(3.6)

The value of  $C_s$  is closely related to the relation of the maximum crack spacing and the minimum spacing, and it seems to take a value between zero and 0.5.

Some numerical example are shown in Fig. 3.2 [8][9][10], comparing the analysis with the experimental data of the uniaxially tensioned RC members. In the figure, the shaded area is bounded by the upper and the lower envelop curves. Good agreement is observable from the figures.

We develop now the theory into two dimensional stress field assuming linear bond slip laws. Nonlinearity is again taken into consideration by the similar, but, expanded modification factors,  $^{\beta}x$  and  $^{\beta}y$  to the X and Y directions. However, our discussion is limited to cases where cracks are formed in one direction only or to two orthogonal directions in alignment with two orthogonal reinforcement directions, in which case the tension stiffening effects in each direction are treated independently.

Taking out one portion of a cracked panel which is separated by the two cracks as shown in Fig.3.3(a), it is possible to consider that the strips which are the tributary area of both steel reinforcements for the X direction and the Y direction as shown in Fig.3.3(b), independently satisfy the bond slip law along the X and Y directions. The concrete stresses at a square where the strips overlap are then estimated by the similar procedure as we did in the derivation of Eq.(3.2). For the X direction,

$$\sigma_{c,x} = \frac{p_x \sigma_{s,x}}{(1+np_x)} \left\{ 1 - \frac{\cos h(x/b_{c,x})}{\cos h(\ell_{c,x}/b_{c,x})} \right\}$$
(3.7a)

and similarly for the Y direction,



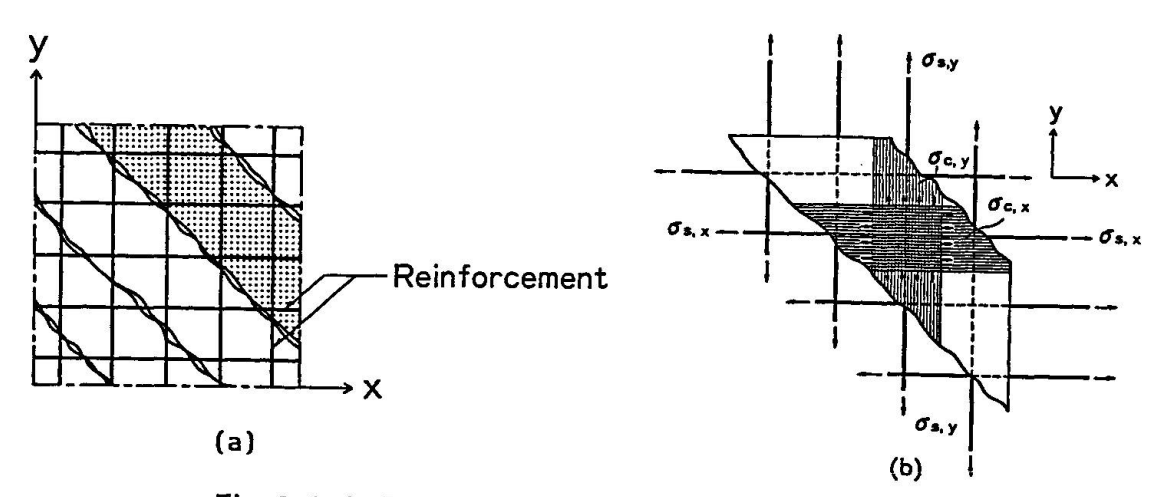


Fig. 3.3 A Cracked Reinforced Concrete Panel

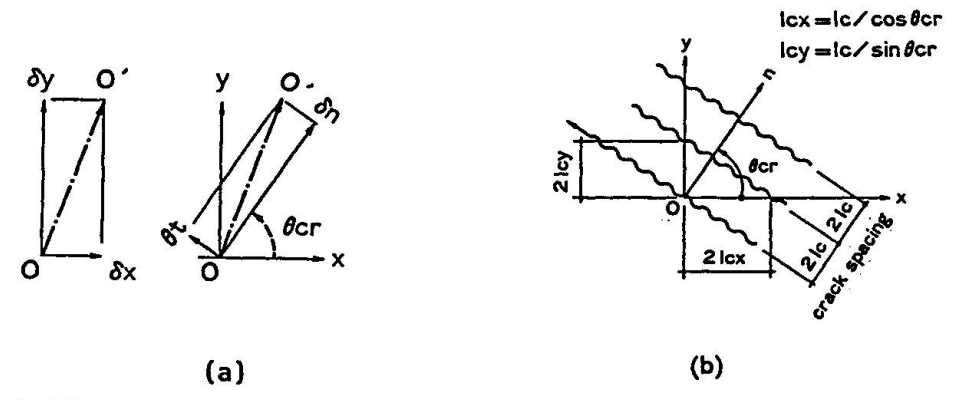


Fig. 3.4 Crack Widths to the (x,y) and (n,t) Directions and Crack Spacings of Parallel Cracks

$$\sigma_{c, y} = \frac{p_{y} \sigma_{s, y}}{(1 + np_{y})} \left\{ 1 - \frac{\cos h (y / b_{c, y})}{\cos h (\ell_{c, y} / b_{c, y})} \right\}$$
(3.7b)

where  $\sigma_s$ ,x and  $\sigma_s$ ,y are steel stresses at a crack and are equal to the first principal stress of applied stresses from the assumption of lattice structures and  $\rho_x$  and  $\rho_y$  are the reinforcement ratios to the X and Y directions. The values 1c and bc with suffix x or y denote the crack spacings and the bond characteristics to the X or Y directions.

The stresses of Eq.(3.7a) and Eq.(3.7b) compose total stresses together with the compressive stress in the concrete struts working to the direction parallel to the cracks. Principal stresses are decided by their stresses. However, in simplicity, the first principal stress may be approximated as

$$\sigma_{t} = f_{1}(\theta) \sigma_{c,x} \max + f_{2}(\theta) \sigma_{c,y} \max$$

$$f_{1}(\theta) = \cos^{n} \theta_{cr}, \quad f_{2}(\theta) = \sin^{n} \theta_{cr}$$
(3.8)
$$(3.9a, 3.9b)$$

The value of n of Eq.(3.9) depends on the crack angle, the relative location of reinforcements and so forth, however, n=2 is assumed in this study. The crack spacing and applied stress relation is then expressed as

$$f_{1}(\theta) = \frac{p_{x} \sigma_{S,x}}{(1+np_{x})} \left[1 - \operatorname{sech}\left(\frac{\ell_{c}}{b_{c,x} \cos \theta_{cT}}\right)\right] + f_{2}(\theta) = \frac{p_{y} \sigma_{S,y}}{(1+np_{y})} \left[1 - \operatorname{sec} h \frac{\ell_{c}}{b_{c,y} \sin \theta_{cT}}\right] = f_{t} (3.10)$$



Crack widths or slipping off of reinforcements at a crack,  $\delta_x$  ·  $\delta_y$  are then given as

$$\delta_{x} = 2b_{c,x} \tan h \left( \ell_{c,x} / b_{c,x} \right) \frac{\sigma_{s,x}}{p_{x} E_{s}}$$

$$\delta_{y} = 2b_{c,y} \tan h \left( \ell_{c,y} / b_{c,y} \right) \frac{\sigma_{s,y}}{p_{y} E_{s}}$$
(3.11)

On the other hand, the geometry of the crack in Fig.3.4(b) gives the following relation in the (n,t) coordinate system.

and by definition, crack strain is given as

$$\begin{Bmatrix} \varepsilon_{n} \\ \tau_{nt} \end{Bmatrix} = \begin{bmatrix} 1 & 1 \\ -\tan \theta_{cr} \cot \theta_{cr} \end{bmatrix} \begin{bmatrix} \lambda_{x}/\rho_{x} E_{s} & 0 \\ 0 & \lambda_{y}/\rho_{y} E_{s} \end{bmatrix} \begin{Bmatrix} \sigma_{s,x} \\ \sigma_{s,y} \end{Bmatrix} = \begin{bmatrix} S \end{bmatrix}_{nt} \begin{Bmatrix} \dot{\sigma}_{1} \\ \dot{\sigma}_{2} \end{Bmatrix}$$
(3.13)

where 
$$(S)_{nt} = \begin{bmatrix} 1 & 1 \\ -\tan\theta_{cr} & \cot\theta_{cr} \end{bmatrix} \begin{bmatrix} \lambda_x/p_x E_s & 0 \\ 0 & \lambda_y/p_y E_s \end{bmatrix} \begin{bmatrix} 1 & 0 \\ 1 & 0 \end{bmatrix}$$

As has been in the uni-dimensional cases, the tension stiffening effect is evaluated by the value of  $\lambda_x$  and  $\lambda_y$ . If  $^{\lambda}x$ ,  $^{\lambda}y$  =0, full contribution to tension stiffness exists from concrete while if  $^{\lambda}x$ ,  $^{\lambda}y$  =1, no tension stiffness effect exists, and the transition from  $^{\lambda}x$ ,  $^{\lambda}y$  =0 to  $^{\lambda}x$ ,  $^{\lambda}y$  =1 is dependent on steel stress and other nonlinearity factors, and  $\mu_x$ ,  $^{\mu}y$  which are the normalized crack spacings, are modified by the nonlinear factors  $\beta_x$ , and  $\beta_y$ .

Once we obtain the form of Eq.(3.13), it is possible to construct a damage tensor due to cracking. As applied stress  $\{\sigma\}$  equals the sum of  $\{D\}_s\{\varepsilon\}_t$  and  $\{D\}_c\{\varepsilon\}_e$  [11],

$$\{\varepsilon\}_{cr} = (S)(D)_{c}\{\varepsilon\}_{e} + (S)(D)_{s}\{\varepsilon\}_{t}$$
(3.14)

and as total strain,  $\{\varepsilon\}_t=\{\varepsilon\}_z+\{\varepsilon\}_{cr}$  ,  $\{\varepsilon\}_e$  being the elastic strain,

$$(I - \{s\} \{D\}_s) \{\varepsilon\}_t = (\{s\} \{D\}_c + I) \{\varepsilon\}_e$$
(3.15)

Substitution of  $\{\varepsilon\}_e$  of Eq.(3.15) to Eq.(3.14) yields,

$$\{\varepsilon\}_{cr} = (A)\{\varepsilon\}_{t} \tag{3.16}$$

where

$$(A) = (S) (D)_S + (S) (D)_C ((S) (D)_C + I)^{-1}$$
(3.17)

Although we can not obtain the inverse of  $\{S\}$ , the equation is reduced to the following form,

$$(A) = ((S)^{-1} + (D)_c^{-1})^{-1} ((D)_c + (D)_S)$$
(3.18)



Then from Eq.(2.9),

$$(\mathcal{Q})_{D_1}^{S} = (D)_{C} \left[ (S)^{-1} + (D)_{C}^{-1} \right]^{-1} ((D)_{C} + (D)_{S}) (D)_{C}^{-1}$$
(3.19)

However, the stress increase will give rise to the damage in concrete in the compression zone. Hence, another damage tensor  $\{\mathcal{Q}\}_{p_2}$  should be considered. If we assume the independency of  $\{\mathcal{Q}\}_{p_1}$  and  $\{\mathcal{Q}\}_{p_2}$ ,  $\{\mathcal{Q}\}_{p_2}$  is separately derived and the modified  $\{\mathcal{Q}\}_{p_2}$  discussed in [12] is used in the following discussion. So for the frictionless mode of displacement of a concrete panel the following constitutive equation is derived.

$$\{\sigma\} = (I - \mathcal{Q}_{\rho_1}^s - \mathcal{Q}_{\rho_2} + \mathcal{Q}_s) (D)_c \{\varepsilon\} = (I - \mathcal{Q}_s) (D)_c \{\varepsilon\}$$
(3.20)

where  $(Q_R) = (D_S) (D_C)^{-1}$  from Eq. (2.11).

When we consider the uniaxial condition and neglect the Poisson's ratio of concrete, Eq. (3.19) is reduced to

$$Q_{p_1} = \frac{1 + np}{1 + \frac{np}{\lambda}} \tag{3.21}$$

and the factor  $\lambda$  represents the tension stiffening effect as well. For pure shear loading condition to a panel with equal reinforcement to the X and Y directions, Eq.(3.19) is again reduced to the same equation as

$$(Q)_{o_1} = \begin{bmatrix} \frac{1+np}{1+\frac{np}{2}} & 0 & 0 \\ 0 & 0 & 0 \end{bmatrix}$$
 (3.22)

The derived constitutive equation is applicable to cases where there is no frictional slip at a crack. This situation can be seen for example in the plane subjected unidirectional load or pure shear load.

In Fig.3.5, the comparison of the experimental data by Vecchio, and Collins [13] is shown with the calculated values. In these figures,  $\lambda$  con denotes the factor to be multiplied to the  $\epsilon_0$ , the strain that corresponds to the maximum compressive stress of concrete. The figures show the tension stiffness effect as well as the shear rigidity. The agreement is reasonable.

## 4. CONSTITUTIVE EQUATIONS OF CRACKED RC PANELS FOR THE FRICTIONAL MODE

When the concrete has lateral differential movement of two surfaces at a crack as shown in Fig.4.1, the shear dilatancy and shear friction give rise to complicated problems, and the relations between crack opening,  $\delta_n$ , and crack slip,  $\delta_t$ , versus shear stress,  $\tau_{nt}^c$ , and normal stress,  $\sigma_n^c$ , at a crack are still in argument. Bazant and Ganbaroba [3] discussed the characteristics of this and obtained mathematical expressions for each term of the [B] matrix, the stiffness matrix which relates  $(\sigma_n^c, \tau_{nt}^c)$  and  $(\delta_n, \delta_t)$ , from intuitive consideration of the general properties of crack stiffness satisfying singularity conditions at  $(\delta_n, \delta_t) = (0, 0)$ . Recently, Yoshikawa [14] developed a mathematical expression for the [B] matrix from quite a different angle and successfully identified the term from the regression of experimental data.

Referring to the notation in Fig.4.1, the tangential displacement  $\delta_t$  and normal stress,  $\sigma_n$ , due to the shear stress and shear dilatancy effects are written in the following form.



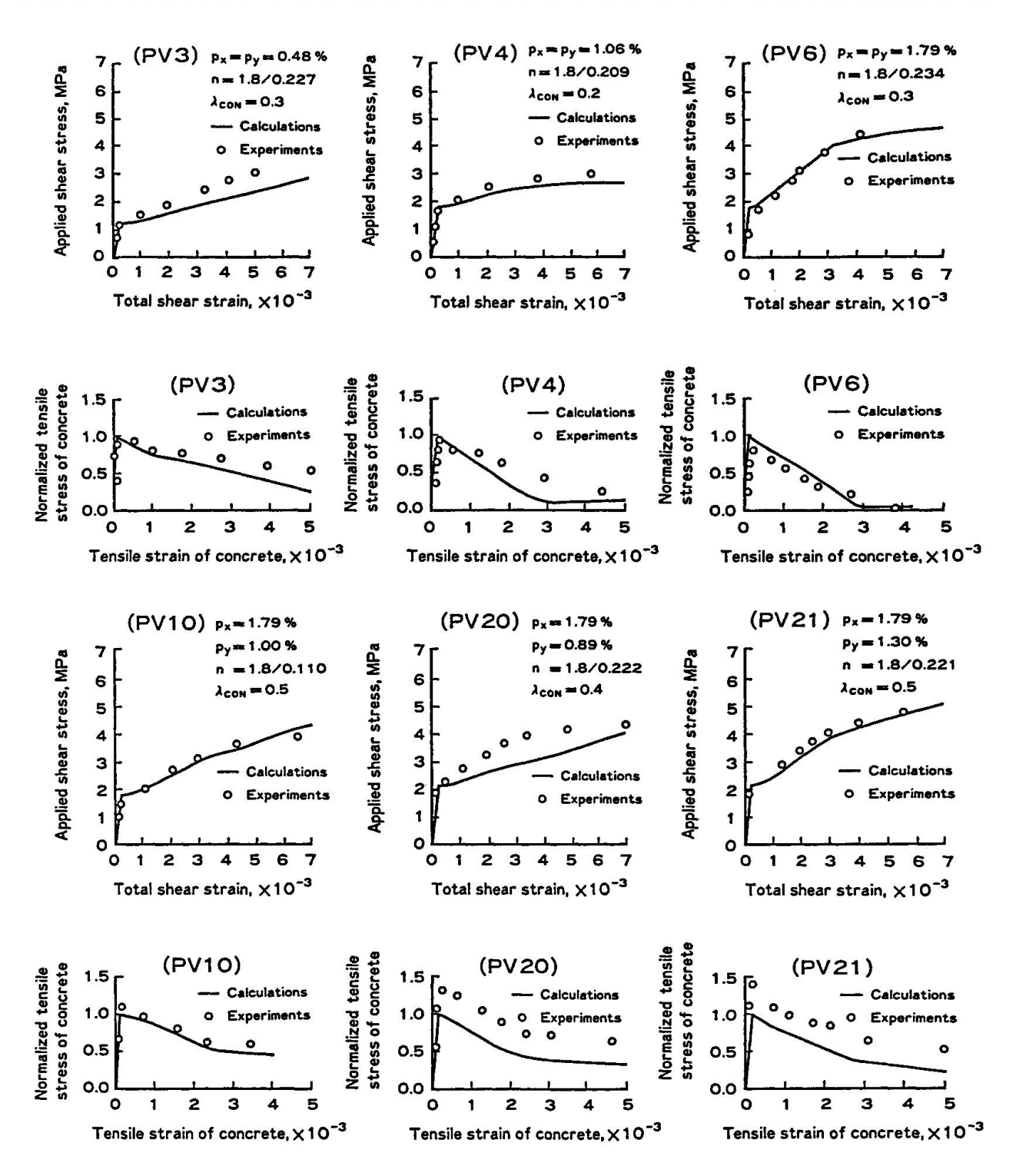


Fig. 3.5 Calculated Tension Stiffness Effects and Shear Rigidity Compared with The Experiments by Vecchio and Collins (Ref. 13)



$$\delta_t = \delta_t (\tau_{nt}^c, \delta_n)$$

$$\sigma_n^c = \sigma_n^c (\tau_{nt}^c, \delta_n)$$
(4.1)

The total differential of  $\delta_t$  and  $\delta_n$  is written as

$$d \, \delta_t = \frac{\partial \, \delta_t}{\partial \, \tau_n^{\, c}} \cdot d \, \tau_{nt}^{\, c} \, + \frac{\partial \, \delta_t}{\partial \, \delta_n} \, \cdot d \, \delta_n$$

$$d\sigma_n^c = \frac{\partial \sigma_n^c}{\partial \tau_{nt}^c} \cdot d \tau_{nt}^c + \frac{\partial \sigma_n^c}{\partial \delta_n} \cdot d \delta_n$$

$$(4.2)$$

In Eq.(4.2), the term  $\frac{\partial \tau_{nt}^c}{\partial \delta_n}$  or its inverse do not appear, making the kinematical understanding much easy. However, the form itself is somewhat unusual since one displacement and one

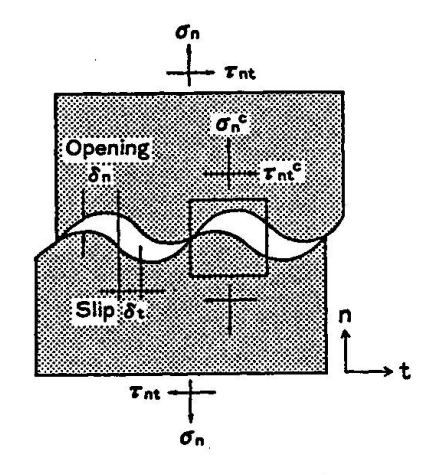


Fig. 4.1 Conceptual Figures of Displacements and Stresses at a Crack

stress component are functions of another displacement and stress components. However, the four terms appearing as derivatives of Eq.(4.2) are clearly defined physically. (  $\partial \delta_t / \partial \tau_{nt}^c$ )  $\delta_n^{-1} = k_t$  is the shear rigidity at a crack, (  $\partial \delta_t / \partial \delta_n$ )  $\tau_{n} = const$  =  $\beta_d$  is the dilatancy ratio, (  $\partial \sigma_n^c / \partial \delta_n$ )  $\tau_{n} = const$  =  $k_n$  is the rigidity to the normal direction of a crack, and (  $\partial \sigma_n^c / \partial \tau_{nt}^c$ )  $\delta_n = const$  =  $(-\mu_f)^{-1}$  is the frictional coefficient. These four values are rather easily determined from the comparison of the experimental results.

Eq(4.2). is rewritten in the normal form as,

$$d \tau_{nt}^{c} = \left[ 1 / \left( \frac{\partial \delta_{t}}{\partial \tau_{nt}^{c}} \right) \right] d \delta_{t} - \left[ \left( \frac{\partial \delta_{t}}{\partial \delta_{n}} \right) / \left( \frac{\partial \delta_{t}}{\partial \tau_{nt}^{c}} \right) \right] d \delta_{n}$$

$$d \sigma_{n}^{c} = \left[ \left( \frac{\partial \sigma_{n}^{c}}{\partial \tau_{nt}^{c}} \right) / \left( \frac{\partial \delta_{t}}{\partial \tau_{nt}^{c}} \right) \right] d \delta_{t} - \left[ \frac{\partial \sigma_{n}^{c}}{\partial \delta_{n}} - \left( \frac{\partial \sigma_{n}^{c}}{\partial \tau_{nt}^{c}} \cdot \frac{\partial \delta_{t}}{\partial \delta_{n}} \right) / \left( \frac{\partial \delta_{t}}{\partial \tau_{nt}^{c}} \right) \right] d \delta_{n}$$

$$(4.3)$$

or the inverse relation is similarly obtained. Eight different terms of partial derivatives are related to each other as shown in Eq.(4.4).

$$\begin{bmatrix}
\frac{\partial \delta_t}{\partial \tau_{nt}^c} & \frac{\partial \delta_t}{\partial \delta_n} \\
-1/\mu_f & k_n
\end{bmatrix}
\begin{bmatrix}
k_t & \frac{\partial \tau_{nt}^c}{\partial \sigma_n} \\
\beta_d' & \frac{\partial \delta_n}{\partial \sigma_n}
\end{bmatrix} = \begin{bmatrix}
1 & 0 \\
0 & 1
\end{bmatrix}$$
(4.4)

As four other partial derivatives are obtained from Eq.(4.4), Eq.(4.3) is rewritten in the form of

$$\begin{bmatrix} d \tau_{nt}^{c} \\ d \sigma_{n}^{c} \end{bmatrix} = k_{t} \begin{bmatrix} 1 & -(1-\xi)/\beta_{d} \\ -1/\mu_{f} & 1/(\mu_{f}\beta_{d}) \end{bmatrix} \begin{Bmatrix} d \delta_{t} \\ d \delta_{n} \end{Bmatrix}$$
(4.5)

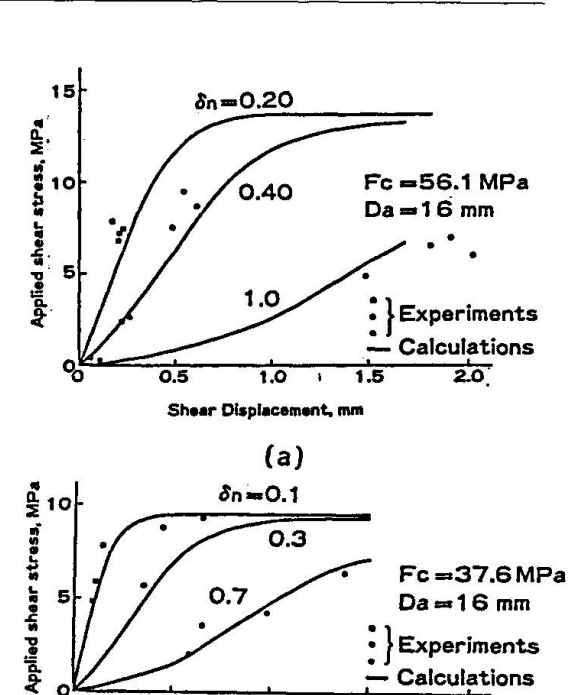
or inversely,

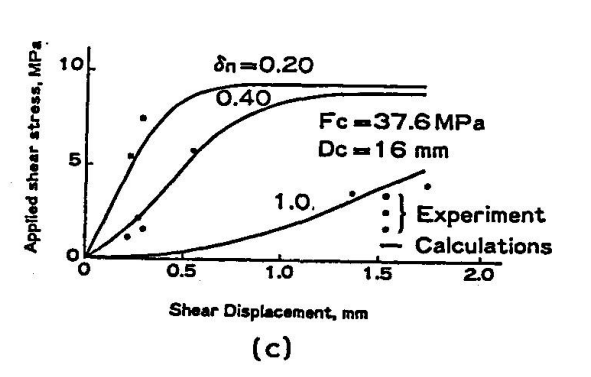
Experiments Calculations



Table 4.1 Identification by Yoshikawa of kt, kn,  $\mu_f$ , and  $\beta_d$  Values at A Crack

F	
SHEAR STIFFNESS: kt [MPa/mm]	CONSTANTS
$\begin{aligned} & k_t = K_{\text{IST}} \operatorname{sech}^2 \left\{ \frac{K_o}{\tau_u} \left( \delta_t - \delta_{t1} \right) \right\} \\ & K_{\text{IST}} = a_1 \left( \frac{f_c}{25} \right)^{a_2} \left( \frac{D_a}{16} \right)^{a_3} \delta_n^{-a_4} \\ & \delta_{t1} = a_5 \left( \frac{f_c}{25} \right)^{a_6} \left( \frac{D_a}{16} \right)^{-a_7} \delta_n^{-a_8} \\ & \tau_u = \tau_o \frac{a_9}{a_{10} + \left( \delta_n / D_a \right)^{a_{11}}} \\ & \tau_o = a_{12} f_c \\ & K_o = K_{\text{IST}} (1 + q) \\ & q = \tan h \left( \frac{K_o \delta_{t1}}{\tau_u} \right) \end{aligned}$	$a_1 = 3.74, a_2 = 0.60$ $a_3 = 0, a_4 = 0.96$ $a_5 = 1.42, a_6 = 0$ $a_7 = 1.20, a_8 = 1.31$ $a_9 = a_{10} = 0.01$ $a_{11} = 2$ $a_{12} = 0.2 \sim 0.3$ (0.245)  Da: The Maximum Aggregate Size
NORMAL STIFFNESS:kn [MPa/mm]	CONSTANTS
$K_n = b_1 b_2 (\delta_n - \delta_d \delta_t)^{-(b_2+1)}$	b <sub>1</sub> = 0.0082 b <sub>2</sub> = 0.878
FRICTIONAL RATIO: #1	CONSTANTS
$\mu_1 = c_1 \mu_0 \exp(c_2 \delta_n)$	$\mu_0 = 1.16$ $c_1 = 0.5 \sim 1.5$ $c_2 = 0.61$
DILATANCY RATIO : 8d	CONSTANTS
$\beta_d = c_3 \beta_0 \exp\left(-c_4 \left  \frac{\sigma_0^c}{f_c} \right  \right)$	$\beta_0 = 1.64$ $c_3 = 0.5 \sim 1.5$ $c_4 = 6.42$





1.0 Shear Displacement,

Fig. 4.2 The Shear Rigidity at A Crack by Reinhardt and Walraven (Ref. 15)

where  $\beta_d = \beta'_d/(1 + \mu_f \beta'_d k_n / k_t)$  and  $\xi = \mu_f \beta_d k_n / k_t$ 

A detailed discussion of the characteristics of the equation is found in the paper [14]. The identified values by Yoshikawa are shown in Table 4.1 and used in the following numerical calculations.

We will now develop the constitutive equations for the frictional displacement field. We rewrite Eq.(4.5) as the relation of total displacements and total stresses in the following form.

where



where  $\mu \cdot b_c$  is the average crack spacing as shown in Eq.(3.5). We transform it for the relation in the global coordinate system using transformation matrices  $T_1$  and  $T_2$  for stress and engineering strain as

$$\{\sigma\} = (T_1)^{-1} \{\Delta\} (T_2) \{\varepsilon\}_{cr} = (F) \{\varepsilon\}_{cr}$$

$$(4.8)$$

On the other hand, the concrete portion which does not contain a crack has elastic rigidity and the stress equilibrium at a crack gives the relation,

$$(F) \{ \varepsilon \}_{cr} = (D)_c \{ \varepsilon \}_e \tag{4.9}$$

The crack strains are derived in terms of total strains from Eq.(4.8) and Eq.(4.9) as

$$\{\varepsilon\}_t = \{\varepsilon\}_{cr} + \{\varepsilon\}_e = \left((D)_c^{-1}(F) + I\right)\{\varepsilon\}_{cr}$$
(4.10)

The damage tensor can be derived in the form of Eq.(4.11), referring to Eq.(2.8).

$$(\mathcal{Q})_{D_1}^F = (D)_c \Big( (D)_c^{-1}(F) + I \Big)^{-1} (D)_c^{-1} = (D)_c \Big[ (F) + (D)_c \Big]^{-1}$$
(4.11)

If the concrete remains elastic except for the cracked area,  $(2)_{p_1}'$  of Eq.(4.11) is the only tensor that constitutes the equation; however, as the concrete rigidity is reduced due to the high intensity of compressive stress, we need another damage tensor. Using the series model, total strain is written with the damage strain,  $\{\varepsilon\}_{cd}$ , due to compressive stress as

$$\{\varepsilon\}_t = \{\varepsilon\}_{e} + \{\varepsilon\}_{cr} + \{\varepsilon\}_{cd} \tag{4.12}$$

and

$$\{\varepsilon\}_{cd} = (D_c)^{-1} (\Omega)_{\rho_2} (D_c) \{\varepsilon\}_t \tag{4.13}$$

Equation (4.8) with Eq. (4.12) and Eq. (4.13) yields

$$\{\varepsilon\}_{cr} = (F) + (D)_c^{-1} (D)_c (I - (D)_c^{-1} (Q)_{\rho_2} (D)_c) \{\varepsilon\}_t$$
(4.14)

Hence,

$$(Q)_{p_1}^F = (D)_c ((F) + (D)_c)^{-1} (I - (Q)_{p_2})$$
(4.15)

The total constitutive equations are derived as

$$\{\sigma\} = (I - \mathcal{Q}_{\rho_1}^{\prime} - \mathcal{Q}_{\rho_2} + \mathcal{Q}_{R}) [D]_{c} \{\varepsilon\} = (I - \mathcal{Q}_{S}) [D]_{c} \{\varepsilon\}$$

$$(4.16)$$

However,  $(\mathcal{Q})_{p_1}$  is dependent on  $(\mathcal{Q})_{p_2}$ . The applicability of this is examined by comparison with the experiment of panels by Reinhardt and Walraven [15], as shown in Fig.4.2. Agreement seems reasonable.

## 5. CONSTITUTIVE EQUATIONS OF CRACKED RC PANELS FOR THE MIXED MODE

In stress conditions when the crack spacing is comparatively wide and frictional displacement at cracks occurs, the mixed mode of displacement takes place. In other words, the concrete close to the cracks is stressed in compression to the normal direction to a crack surface while the region away from the crack is



stressed in tension. Hence it is considered that the constitutive equation for stress fields of this kind is expressed by the combination of Eq.(3.18) and Eq.(4.16). However, the combination is dependent on a situation which may be classified according to the number of crack orientations, the number of reinforcement orientations, and their relative angles, as the tension stiffening effect in a steel is greatly affected by the occurrence of crossing of cracks in a bar.

In this paper, the following two cases are discussed. The first one is the case in which all cracks are unidirectional. For the cracked reinforced concrete element, the shear forces and normal forces are supposed to be applied. Taking out a representative portion between two cracks it is possible to separate the concrete into two portions, one in which compressive force is working to the normal direction for crack surfaces and the other portion where tensile stress is working to the normal direction for cracked surfaces as shown in Fig.5.1(b).

The transition point of the normal stress from the minus sign (compression) to the plus sign (tension) is again approximated by the linear solution of the governing equation of  $d^2g/d^2\xi-k$  g=0 with boundary conditions of  $\sigma_{\mathcal{S},\ \xi}=\sigma_{\mathcal{S},\ \xi}^{\ b}$  and  $\sigma_{c,\ \xi}=\sigma_{c,\ \xi}^{\ b}$  at a crack, where the  $\xi$  direction is normal to crack surfaces. Solving the equation, concrete stress is expressed as

$$\sigma_{c,\xi} = -\frac{s \cdot k}{A_c} \cdot \frac{u_0}{g_0} \left( \frac{\sigma_{s,\xi}^b}{E_s} - \frac{\sigma_{c,\xi}^b}{E_c} \right) \left\{ \cos h \left( \frac{\xi}{b_c} \right) - 1 \right\}$$
(5.1)

where s,  $u_0$ , and  $g_0$  again denote the perimeter of a bar, the bond strength and the bond slip corresponding to  $u_0$ , respectively, and  $k = (u/u_0)/(g/g_0)$ . Ac denotes sectional area of tributary concrete section of a bar.

The location where concrete stress changes from compression to tension is written as

$$\xi = b_c \cos h^{-1} C_1$$

$$C_{1} = \cos h \left(\frac{\ell_{c}}{b_{c}}\right) + A_{c} \sigma_{c, \xi}^{b} / \left[\frac{s k u_{0}}{g_{0}} \left(\frac{\sigma_{s, \xi}^{b}}{E_{s}} - \frac{\sigma_{c, \xi}^{b}}{E_{c}}\right) \frac{b_{c}^{2}}{\cos h \left(\ell_{c}/b_{c}\right)}\right]$$
(5.2)

If  $C_1 < 1$ , there exists no tension zone and only the frictional mode exists. However, if  $C_1 > 1$ , the displacement is always in the mixed mode. The portion where concrete is stressed in tension to the  $\xi$  direction, has to be treated as having slip between steel and concrete and its situation is exactly same as the case mentioned in section 3. We Separate the concrete portion along the  $\xi$ 

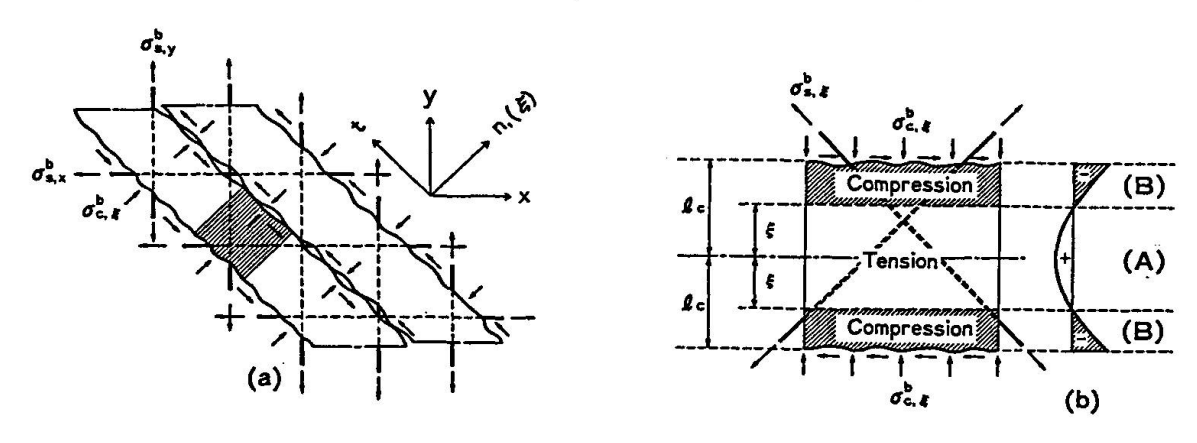


Fig. 5.1 Stress Condition at a Crack in the Mixed Mode Displacement Condition



direction to the region A where  ${}^{\sigma}\xi$  is in compression and, to the region B where  ${}^{\sigma}\xi$  is in tension. The concrete stress is zero at the boundary between A and B. Hence we can consider that the constitutive equation of Eq.(3.20) which considers tension stiffness is applicable in the region A.

The slipping out of a bar at the region A contributes to the crack opening of the region B. Hence the total crack opening,  $\delta_n$ , should be the sum of the contributions from the region A and from the region B.

$$\delta_n = \delta_{n...} + \delta_{n...} \tag{5.3}$$

Basing on these consideration, we can develop the constitutive equations for the mixed mode. For the region B, the constitutive equations developed for the frictional mode are applicable. Obviously, at the boundary of two regions, the stress equilibrium should be satisfied. Hence  $\{\sigma\}_{A}^{b} = \{\sigma\}_{B}^{b}$ , and the total elongation of the portion between two cracks is the sum of the elongation of each region of A and B, and the average strain of the total portion  $\{\varepsilon\}_{t}$  is written as

$$\begin{Bmatrix} \varepsilon_{n} \\ \varepsilon_{t} \\ r_{nt} \end{Bmatrix} = \begin{bmatrix} \eta & 0 & 0 \\ 0 & 1 & 0 \\ 0 & 0 & \eta \end{bmatrix} \begin{Bmatrix} \varepsilon_{n} \\ \varepsilon_{t} \\ r_{nt} \end{Bmatrix} + \begin{bmatrix} 1-\eta & 0 & 0 \\ 0 & 0 & 0 \\ 0 & 0 & 1-\eta \end{bmatrix} \begin{Bmatrix} \varepsilon_{n} \\ \varepsilon_{t} \\ r_{nt} \end{Bmatrix} = [\eta] \{\varepsilon\}_{A} + [\zeta] \{\varepsilon\}_{S} \tag{5.4}$$

where,  $\eta$  is the fraction to the crack spacing of the length of the area where the concrete is in compression along the  $\xi$  direction and frictionless mode is predominant. This is written in the linear case as

$$\eta = \frac{\xi}{\ell_c} = \frac{1}{\mu_c} \cos h^{-1} C_1 \tag{5.5}$$

As we already have the constitutive equations (3.20) and (4.16) for the regions A and B, Eq.(5.4) is rewritten as

$$\{\varepsilon\}_{t} = (\eta) [D]_{c}^{-1} (I - Q_{A})^{-1} \{\sigma\} + (\zeta) [D]_{c}^{-1} (I - Q_{B})^{-1} \{\sigma\}$$
 (5.6)

Hence,

$$\{\sigma\} = (M) \{\varepsilon\}_t \tag{5.7}$$

where 
$$(M) = ((\eta)(D)_c (I-(Q)_A)^{-1} + (\zeta)(D)_c^{-1} (I-(Q)_B)^{-1})^{-1}$$

It should be noted that we can not have the frictional mode from the beginning since the crack initiation is always to the principal tensile direction and the first mode should be the frictionless mode. After a small crack width is formed, then the frictional mode or the mixed mode can exist. At the initiation of the first step of the friction mode, the stress equilibrium requires that  $\{\sigma\}_{friction\ less} = \{\sigma\}_{friction\ }$  and the constitutive equation (5.7) of the first step must satisfy this condition.

Experiments corresponding to the mixed mode are very scarce. However, Millard and Jonson [16] carried out this type of experiment using the specimen shown in Fig.5.3(a). They gave rise to a crack at the center of a specimen by applying tensile forces at both ends. Then maintaining the tensile stress, the shear force was applied at the center. The stress condition of concrete will be such that the compressive stress is working at the crack to the normal direction to a crack surfaces while the tensile force is working at the ends to the same direction.

The experimental relations between the shear stress and the shear displacement are shown in comparison with the calculated relations in Fig.5.3(b),(c),(d), and (e). There is some disagreement between them. The calculated values give comparatively softer tendencies compared with the experimental one. These may be due to the assumption of  $\eta$ =0.5. In Fig.5.2, the differences in the shear rigidity due to the extent of the fraction of the region A of the total area were

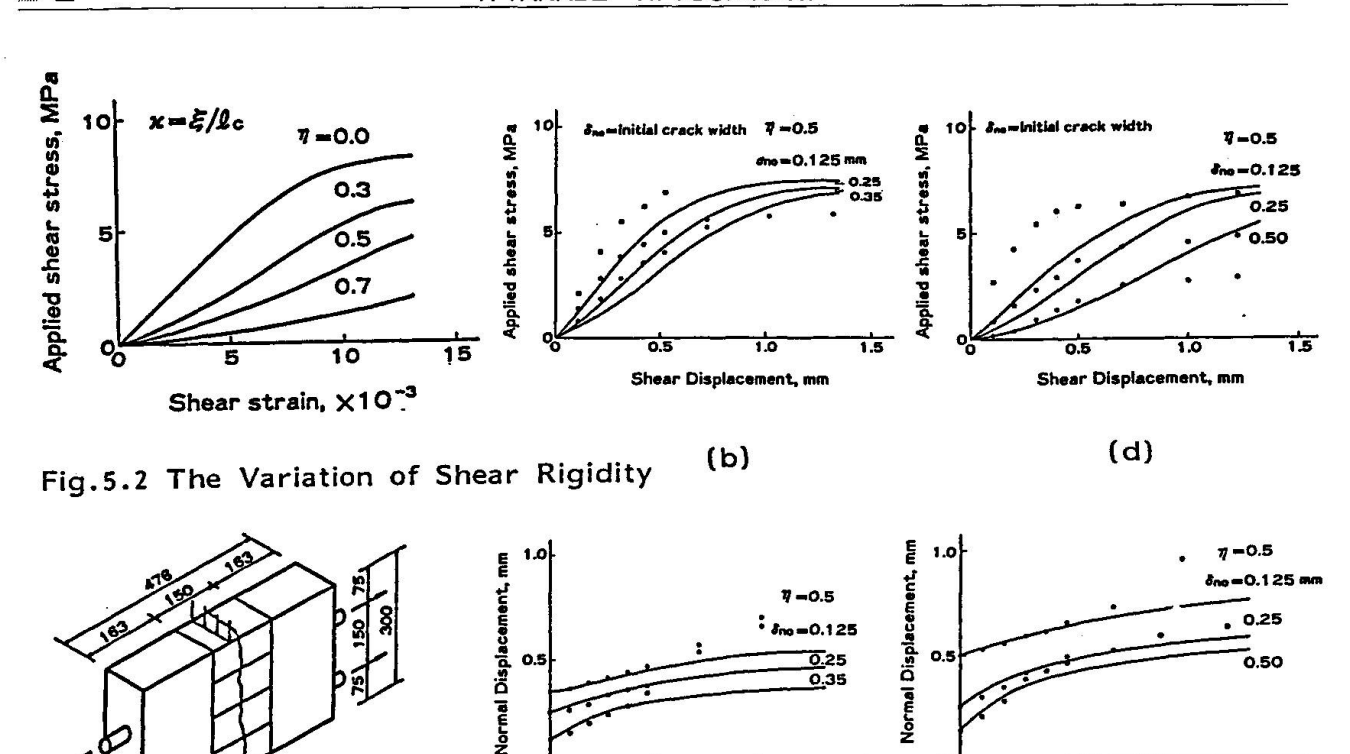


Fig. 5.3 Shear Stress versus Shear Displacement and Normal Displacement Relations by Millard and Johnson (Ref. 16)

Shear Displacement, mm

(c)

shown. The numerical calculations show that the greater the fraction of the region A, the softer is the shear rigidity.

Another case is the case in which we have two orthogonal cracks to the directions of reinforcements as shown in Fig.5.4(a). The mixed mode to the X direction and the Y direction are assumed to be taken independently. In other words, we ignore the interaction of shear displacement friction at the point where four corners from different segments meet.

The only difference from what we derived in the former part of the same section is that shear displacement is affected by the cracks oriented to the X and Y directions. The strain to the normal direction is derived assuming the displacement mode to each direction as the uncoupled mixed mode. Hence,

$$\{\varepsilon\}_{t} = \{C_{M}\}\{\sigma\} \tag{5.8}$$

1.5

Shear Displacement, mm

(e)

$$(C_{M}) = (\eta)_{x} (D)_{c}^{-1} (I - \Omega_{A \cdot x})^{-1} + (\eta)_{y} (D)_{c}^{-1} (I - \Omega_{A \cdot y})^{-1}$$

$$+ (\zeta)_{x} (M)_{x}^{-1} + (\zeta)_{y} (M)_{y}^{-1}$$

$$(5.9)$$

where

(a)

The value of  $\eta_x$  is the fraction of the region where the frictionless mode is



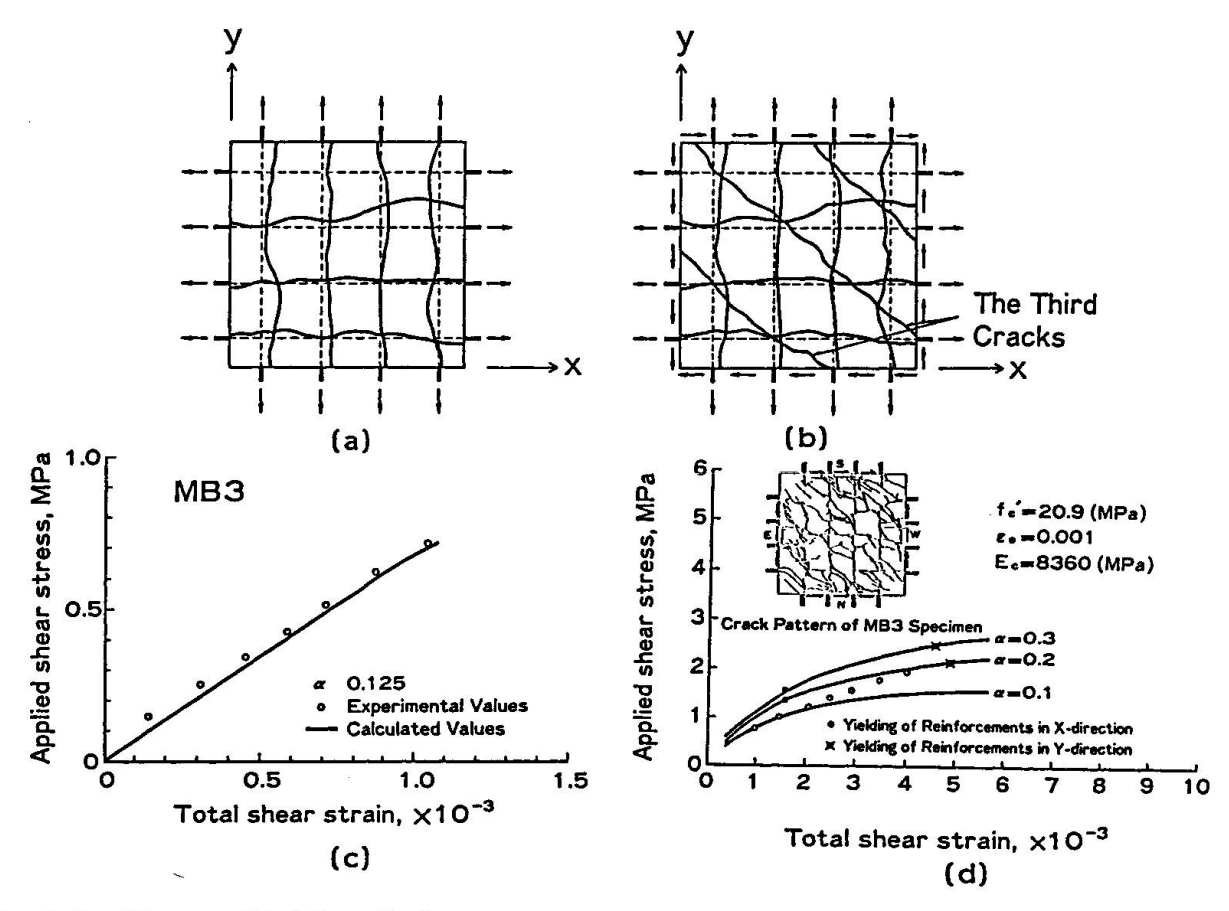


Fig. 5.4 Shear Rigidity Before the Formation of Third Cracks and the Ultimate Strength of MB3 Specimen by Oesterie and Russell (Ref. 17)

predominant to the total region along the X direction, and  $\eta_y$  is defined similarly along the Y direction.

Oesterie and Russell [17] have carried out experiments applying biaxial tension to specimens in the first stage, giving rise to substantial crack width to the X and Y direction, then applying shear force to the point of failure of the specimens, as shown in Fig. 5.4(b). The constitutive Eq. (5.9) is applicable until the third crack is formed to 135° to the X direction. Out of three specimens, two specimens with reinforcement ratios of 0.022 for the X direction and 0.013 for the Y direction were tested by applying loads monotonically. Both showed very similar behavior. For the specimen MB3, crack widths observed at the state when biaxial tension of 5.7 MPa for the X direction and 3.5 MPa for the Y direction were applied were 0.48 mm to the X direction and 0.38 mm to the Y direction, while Eq.(3.20) gives 0.46mm for the X direction and 0.40 mm for the The experiments showed that when the shear force was applied direction. maintaining the last tensile stress level constant, the crack width closed in the Y direction and opened wider in the X direction. Eq.(5.9) also gives the same characteristics. The shear strain and applied shear stress relation during that process is given in Fig.5.4(c), comparing the observed values with the calculated values. In the figure,  $\alpha$  is the parameter which was multiplied to the initial Young's Modulus of concrete in the calculation. At 0.7 MPa of applied shear stress, the third crack, oriented 135° to the X direction, has occurred, and some variation in the shear rigidity was observed. At this stage, Eq. (5.9) is not applicable. However, the ultimate strength may be assessed by



Eq.(3.20) reducing the concrete rigidity which is affected by the three directional crackings. The real line shown in the same figure does not have any meaning other than as a mere estimation of the ultimate strength by the frictionless mode. However, the comparison seems to show that equivalent rigidity of concrete at the cracked condition shown in Fig.5.4(d) is almost 3/10 or less of the initial Young's Modulus of concrete.

#### CONCLUSION

Constitutive equations of composite material of concrete and reinforcement in two dimensional stress field are developed using damage and reinforcement tensors. The derived damage tensors and reinforcement tensors express rationally the tension stiffness effects affected by the reinforcement ratio, bond slip characteristics between concrete and steel, nonlinear deterioration of concrete in compression, and crack stiffness, in which shear dilatancy and shear friction are incorporated. The damage tensors make the nonlinear calculation much easier owing to the fact that  $\mathcal Q$  terms can be treated as initial strains or initial stresses to be accommodated in usual FEM programs.

The constitutive equation for the frictional mode is stable and seems quite dependable as we did not meet any numerical divergence due to the instability of the formulation. However, formulation is limited by the number of the crack orientations and if their number is beyond three and cracks are not parallel to reinforcement, we need to develop a formulation which can simulate the tension stiffening effect for that situation.

#### ACKNOWLEDGEMENT

Authors express their sincere thanks to Dr. S.Hatanaka, and graduate students, Z.S.Wu and D.R.Lokuliyana for their valuable assistance in the numerical calculations as well as in the preparation of the manuscript.

## REFERENCES

- 1. Powell, G.H., DE Villiers, I.P., and Lillon, R.W., Implementation of Endochronic Theory for Concrete with Extensions to Include Cracking, SMiRT 5, Vol.M, Berlin, August, 1979, M2/6.
- 2. Bazant, Z.P., and Gambaroba, P., Rough Cracks in Reinforced Concrete, Journal of the Structural Division, ASCE, Vol. 106, No. ST4, pp.819-842, April, 1980.
- 3. Tanabe, T., Kawasumi, M., and Yamashita, Y., Finite Element Modelling for the Thermal Stress Analysis of Massive Concrete Structures, Proc. of Japan-US Science Seminar on Finite Element Analysis of Reinforced Concrete Structures, Vol. 2, pp. 75-93, Tokyo, May, 1985.
- 4. Yoshikawa, H., and Tanabe, T., A Finite Element Model for Cracked Reinforced Concrete Members Introducing Crack Strain Concept, Proc. of Japan-US Science Seminar on Finite Element Analysis of Reinforced Concrete Structures, Vol.2, pp.237-246, May, 1985.
- 5. Goto, Y., Cracks Formed in Concrete Around Deformed Tension Bars, ACI Journal, Vol. 68, No. 4, pp. 244-251, April, 1971.
- Ozaka,Y., Ohtsuka,K., and Matsumoto,Y., Cracks Formed in Concrete Prism with Axial Tension Bars under Influence of Drying, Concrete Journal, JCI, Vol.23, No.3, pp.109-119, March, 1985.
- 7. Yoshikawa, H., and Tanabe, T., An Analytical Study for the Tension Stiffness of Reinforced Concrete Members on the Basis of Bond Slip Mechanism, Proceedings of JSCE, No. 366, pp. 93-102, V-4, Feb., 1986.



- 8. Yamamoto, Y., Study on Bond Stress of Reinforcements, Crackings and Restoring Characteristics of Embedded Tension Bars (in Japanese), Taisei Technical Report 6, Technical Research Institute, Taisei Corporation, pp.151-193, 1973.
- 9. Somayaji, S., and Shah, S.P., Bond Stress Versus Slip Relationship and Cracking Response of Tension Members, ACI Journal, Vol. 78, No. 3, pp. 217-225, May-June, 1981.
- 10.Rizkalla, S.H., and Hwang, L.S., Crack Prediction for Members in Uniaxial Tension, ACI Journal, Vol.81, No.6, pp.572-579, Nov.-Dec., 1984.
- 11. Tanabe, T., and Lokuliyana, D.R., Constitutive Equations of a Cracked Reinforced Concrete Panel in Frictionless Mode of Displacements, Proceedings of the 43rd Annual Conference of the JSCE, September, 1987 (to be published).
- 12.Vecchio, F., and Collins, M.P., Stress-Strain Characteristics of Reinforced Concrete in Pure Shear, Final Report of IABSE Colloquium on Advanced Mechanics of Reinforced Concrete, pp.211-255, Delft, June, 1981.
- 13. Yoshikawa, H., Analytical Models for the Mechanical Behavior of Reinforced Concrete Members Subjected to Inplane Stresses, Dissertation to University of Tokyo, February, 1987.
- 14.Reinhardt, H.W., and Walraven, J.C., Cracks in Concrete Subjected to Shear, Journal of the Structural Division, ASCE, Vol. 108, No. ST1, pp. 207-224, January, 1982.
- 15.Millard, S.G., and Johnson, R.P., Shear Transfer in Cracked Reinforced Concrete, Magazine of Concrete Research, Vol. 37, No. 130, pp. 3-15, March, 1985.
- 16.Oesterie, H.G., and Russel, H.G., Shear Transfer in Large Scale Reinforced Concrete Containment Elements, Construction Technology Laboratories, NUREG/CR-1374, April, 1980.